Magnetic Resonance: An Introduction to Ultrashort TE (UTE) Imaging

Matthew D. Robson, PhD, Peter D. Gatehouse, DPhil, Mark Bydder, PhD, and Graeme M. Bydder, MB, ChB

Abstract: The background underpinning the clinical use of ultrashort echo-time (UTE) pulse sequences for imaging tissues or tissue components with short T2s is reviewed. Tissues properties are discussed, and tissues are divided into those with a majority of short T2 relaxation components and those with a minority. Features of the basic physics relevant to UTE imaging are described including the fact that when the radiofrequency pulse duration is of the order T2, rotation of tissue magnetization into the transverse plane is incomplete. Consequences of the broad line-width of short T2 components are also discussed including their partial saturation by off-resonance fat suppression pulses as well as multislice and multiecho imaging. The need for rapid data acquisition of the order T2 is explained. The basic UTE pulse sequence with its half excitation pulse and radial imaging from the center of k-space is described together with options that suppress fat and/or long T2 components. Image interpretation is discussed. Clinical features of the imaging of cortical bone, tendons, ligaments, menisci, and periosteum as well as brain, liver, and spine are illustrated. Short T2 components in all of these tissues may show high signals. Possible future developments are outlined as are technical limitations.

Key Words: magnetic resonance imaging, pulse sequences, short T2 tissues, ultrashort echo time

(*J Comput Assist Tomogr* 2003;27:825–846)

The most effective single strategy for diagnosis of parenchymal disease with magnetic resonance (MR) imaging is the use of heavily T2-weighted pulse sequences to detect an increase or decrease in signal from abnormal tissue. Even with newer pulse sequences such as fast spin echo, echo planar imaging, fluid attenuated inversion recovery, and diffusion-weighted imaging, the main diagnostic emphasis remains on detecting signal from tissues with long T2s.

From the earliest days of clinical MR, it was recognized that there were also tissues such as cortical bone which had short T2s.[1,2] The MR signal from these tissues characteristically decays very rapidly, so that with the echo times (TEs) used in conventional clinical imaging, they produce little or no signal and so appear dark.

The low signal from cortical bone and other tissues with a short T2 provides a useful background against which to recognize abnormalities that produce an increase in signal. The disadvantage with this approach is that the absence of signal in the normal tissue means that there is little opportunity to manipulate conspicuity by using different pulse sequences or contrast agents, and that clinically it has not been possible to characterize these tissues in MR terms by, for example, measuring their T1s and T2s.

While tissues such as cortical bone, tendons, ligaments and menisci contain a majority of short T2 components, other tissues also contain short T2 relaxation components, but as a minority species. Signal from the short T2 components in these tissues is not detected with conventional clinical pulse sequences; the MR signal comes from the majority of long T2 components.

In quantitative terms, using conventional two-dimensional Fourier transform (2DFT) imaging with basic spin echo imaging sequences (with TEs down to about 8–10 milliseconds), tissues with T2s shorter than 10 milliseconds have not generally been detectable,[3] although with the shorter TEs in the range of about 1–2 milliseconds now achievable with fast 2DFT gradient echo pulse sequences, the limit of detectability is probably closer to 1–2 milliseconds.

Pulse sequences with even shorter TEs in the range of 0.05–0.20 milliseconds can be produced by use of half radiofrequency (rf) excitations with radial mapping from the center of k-space.[4–22] These ultrashort TE (UTE) pulse sequences have TEs about 10 to 20 times shorter than the shortest generally available on modern clinical systems. With these sequences, cortical bone can be visualized as the highest signal tissue on an image in spite of its very short T2 of 0.42–0.50 milliseconds (Fig.1). What applies to cortical bone also applies

Received for publication June 3, 2003; accepted June 21, 2003.

From the Oxford University Center for Clinical Magnetic Resonance Research, MRS Unit (Dr Robson), John Radcliffe Hospital, Oxford; The Cardiac Magnetic Resonance Unit (Dr Gatehouse), Royal Brompton Hospital, London, England; and Department of Radiology (Dr M. Bydder and G. Bydder), University of California San Diego, San Diego, California.

Reprints: Graeme M. Bydder, Department of Radiology, University of California San Diego, 200 West Arbor Drive, San Diego, CA 92103-8224 (e-mail: gbydder@ucsd.edu).

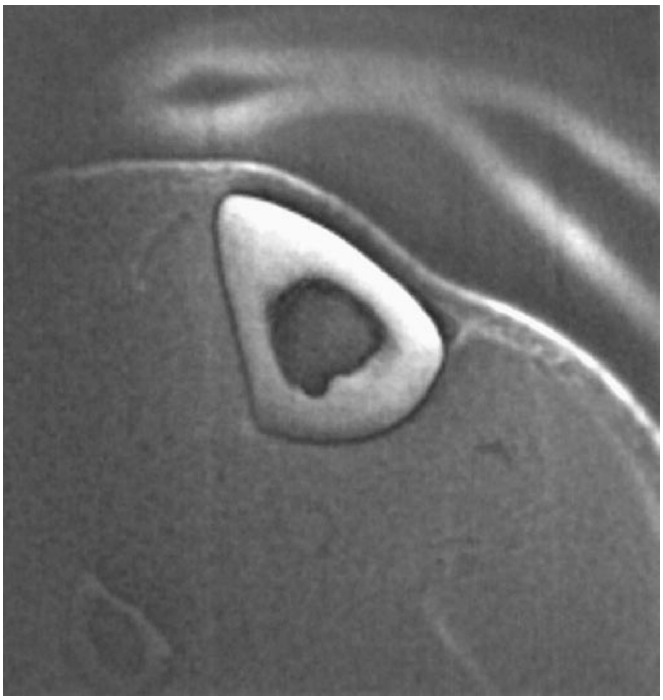

FIGURE 1. Transverse image of a normal tibia: ds STUTE image (TR/TE/TI = 650/0.08 minus 5.95/80 milliseconds) with magnitude reconstruction. The cortical bone is highlighted. It is surrounded by a dark cancellation line and low signal from adjacent muscle and fat. Cortical bone has a shorter T1 (130 milliseconds) than any other tissue in the image.

to other tissues with a majority of short T2 components. In addition, using UTE pulse sequences, signal can specifically be detected from the short T2 components in tissues in which they are in a minority. For reference, ranges of TEs with different pulse sequences are listed in Table 1.

Although the potential of UTE sequences has been apparent for many years, only a limited number of clinical studies of the lung and knee have been published, and less than 20 patients have been reported in the 12 years since the first introduction of these sequences. We have now completed studies of 120 patients with these sequences and have used this experience to review the background underpinning their clinical use in proton imaging.

MR PROPERTIES OF TISSUE

There has been a large volume of work published on the MR properties of tissue, and this section only deals with features of importance for imaging of short T2 components.

The definition of what constitutes a short T2 is not precise. We have taken a short T2 to indicate one that is less than 10 milliseconds. Previously this would have corresponded to the limit of clinical detectability with basic spin echo sequences,[3] but using UTE sequences, most tissues with short T2s are detectable. The lower limit of useful detectability with UTE sequences is likely to be between 0.1 and 0.01 milliseconds, which is two orders of magnitude shorter than the earlier limit of 10 milliseconds and an order of magnitude shorter than that with 2DFT gradient echo images. The limit closely parallels TE. Much of the discussion that follows relates to short T2s in the lower short T2 range down to the limit of detectability with UTE sequences. The term "extremely short" can be applied to tissues that have T2s shorter than this limit, such as those in solids, proteins, and other macromolecules. Estimated mean T2s of some adult tissues and tissue components with short T2s are listed in Table 2.

It is reasonable to assume that all tissues are heterogeneous and have components with different values of T2. For protons, this follows from the fact that tissues contain protons in proteins (with very short T2s of about 10 microseconds, or 0.01 milliseconds) as well as protons in water with much longer T2s. As a first approximation, it is then possible to describe tissues as having both short and long T2 components, although there are probably more than two components in all tissues.

For descriptive purposes, all tissues can then be divided into those with a majority of short T2 components, such as those in Table 3, and those with a minority, which includes most tissues other than those listed in Table 3. The tissues with

TABLE 1. Approximate Range of Pulse Sequence Echo-Times (TEs)

TE Description	TE Values	Examples*
Very long	200 ms and longer	2 DFT, HASTE, fast spin echo, and EPI; very heavily long T2-weighted
Long	20–40 to 200 ms	2 DFT, HASTE, FLAIR, fast spin echo, EPI; heavily long T2-weighted
Intermediate	5–10 to 20–40 ms	2 DFT; T1-weighted or proton density weighted
Short	0.5 to 5–10 ms	2 DFT; T1-weighted
Ultrashort	0.05 to 0.50 ms	Half rf pulse with radial center-out sampling; short T2-weighted

FT = Fourier transform; TR = repetition time. In this paper, the term "ultrashort" has been specifically used to describe radial methods of data acquisition with TEs less than about 0.50 millisecond, although in the literature the terms "ultrashort" and "short" are used less restrictively.

*The weighting depends on the T1 and T2 of the tissue or fluid of interest.

TABLE 2. Approximate Mean T2s of Some Short T2 Tissues and Tissue Components

Tissue or tissue component	Mean T_2
Ligaments	4–10 ms
Achilles' tendon	0.25 and 0.7 ms, 1.2 ± 0.2 ms, 0.53 ms (88%) and 4.8 ms (12%), 7 ms
Knee menisci	5–8 ms
Periosteum	5–11 ms
Cortical bone	0.42–0.50 ms
Dentine	0.15 ms
Dental enamel	70 μs
Protons in water tightly bound to proteins	10 μs
Protons in proteins	10 μs
Protons in solids (eg, calcium hydroxy appatite)	1 μs or less

The sources are adult clinical results and tissue sample results estimated for 1.5 T. Tissues with long T2s such as nasal sinus mucosa which undergo significant dephasing may have short T2*s (<10 milliseconds) and thus appear similar to tissues with short T2s.

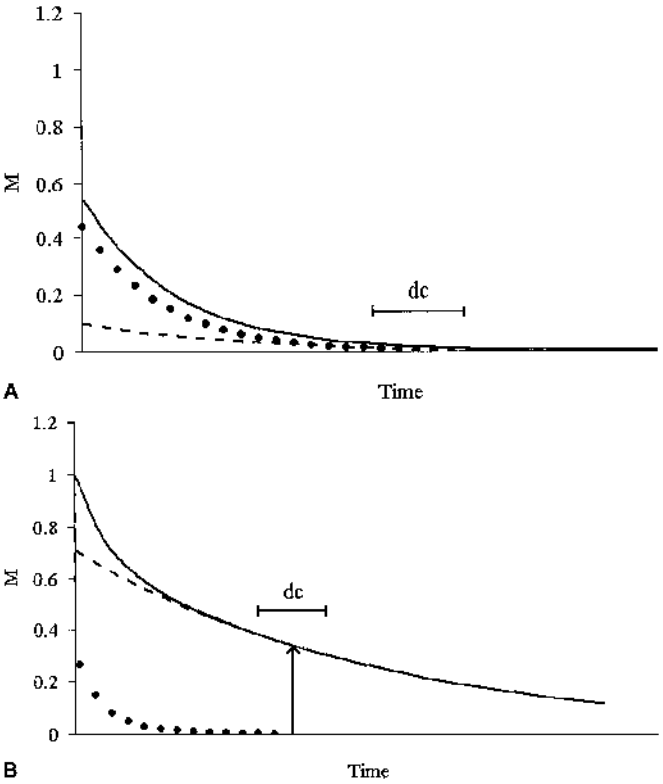

FIGURE 2. Transverse magnetization decay for a tissue with (A) a majority of short T2 components and (B) a minority of short T2 components imaged with a conventional pulse sequence TE. The continuous line represents the total magnetization, the circles that of the short T2 components, and the dashes that of the long T2 components. In (A) the signal has largely decayed to zero by the time of the data collection (dc) at TE and little or no signal is detected. In (B) the magnetization of the short T2 components has decayed to zero by the time of data collection at TE, but that of the long T2 components persists and provides the detectable signal represented by the vertical arrow.

a majority of short T2 components include cortical bone, dentine and enamel (very short T2s and always zero signal with conventional sequences), as well as other tissues where signal is low with conventional sequences but not always zero. The many tissues with a minority of short T2 components such as skeletal muscle and white matter and gray matter of the brain have these components present in low concentrations, typically of about 1% to 20%.[23,24] Magnetization decay curves for these 2 groups of tissues are shown using conventional TE and UTE sequences in Figs. 2 and 3.

There are a number of causes of short T2s in tissues. In general, solids have very short T2s as a result of the strong dipolar interactions between immobile nuclei. Protons in the crystalline component of bone have extremely short T2s (less than 1 microsecond). Protons in macromolecules within membranes or in water closely bound to them are also relatively immobile and have short T2s. Protons in water molecules which are less tightly bound to large molecules have longer T2s eventually extending up to that of free water, which has a T2 of about 4 seconds.

TABLE 3. Normal (Adult) Tissues with a Majority of Short T2 Components

Meninges (dura)	Falx	Tentorium
Membranes	Capsules	Bands
Retinaculi	Septae	Fascae
Sheaths	Nails	Hair
Aponeuroses	Tendons	Ligaments
Menisci	Labrii	Periosteum
Bone	Dentine	Enamel

T2 and T2* effects are indistinguishable using the UTE sequence. A cause for short T2* is susceptibility effects in tissues that are diamagnetic or paramagnetic to different degrees so that their nuclei experience slightly different magnetic fields. This results in a net dephasing with a loss of signal. It is the dominant mechanism for producing short T2*s in a number of situations, particularly those involving paramagnetic species. Diffusion of water molecules in magnetically inhomogeneous tissue will also appear to shorten T2.

Tissues such as tendons and ligaments, which contain a high proportion of linearly ordered collagen are of particular interest. Protons in water bound to collagen in these tissues

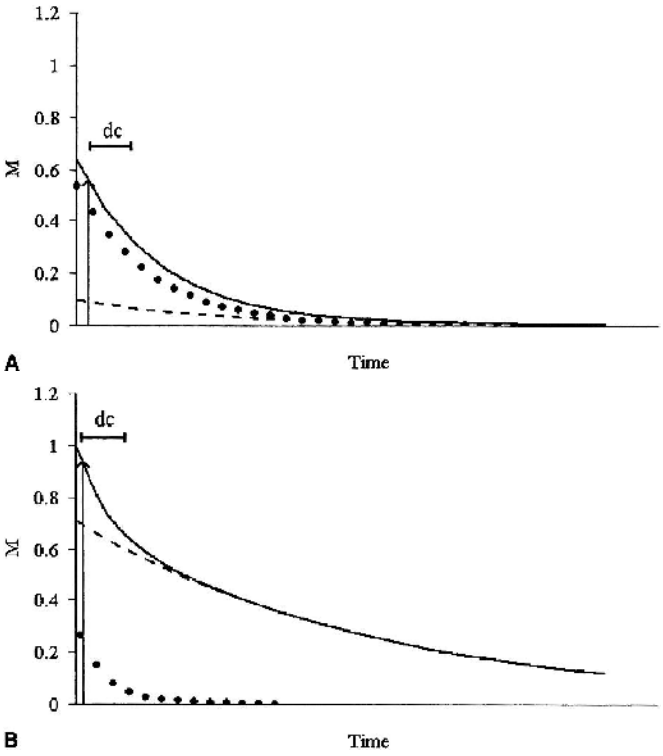

FIGURE 3. Transverse magnetization decay for a tissue with (A) a majority of short T2 components and (B) a tissue with a minority of short T2 components imaged with a UTE pulse sequence with the data collection at a shorter TE and much earlier than in Fig. 2. In comparison to Fig. 2, the magnetization of the short T2 components is now detectable in (A), and magnetization of both the short and long T2 components is detectable in (B).

typically manifest strong dipolar interactions that, unlike those in water bound to proteins in general, are dependent on the macroscopic orientation of the collagen fibers to the static magnetic field, B_o. Their dipolar interactions are modulated by the term $(3\cos^2\theta - 1)$ where θ is the angle the collagen fibers make to B_o. Where $\theta = 55°$, 125°, and so forth (the magic angle), $3\cos^2\theta - 1 = 0$, dipolar interactions are minimized and so T2 is increased. This effect has been recognized as a source of artifact in musculoskeletal imaging where tendons and ligaments may show a high signal when all or part of them happens to be orientated at 55° to B_o.[25] It can also be used as a technique for increasing the T2 of tendons (eg, from 7 to 23 milliseconds[26]) to bring their signal into the detectable range when imaging with conventional spin echo pulse sequence TEs.[27,28]

Although lung was the first tissue imaged with UTE pulse sequences, it is a rather special case. It has a low proton density, is particularly prone to susceptibility effects at lung-air interfaces, a large proportion of the signal comes from flowing blood, and it is subject to respiratory motion. These make imaging of its short T2 components a considerable technical challenge.

In disease, a variety of processes may increase the signal from short T2 components; for example, chronic fibrosis, calcification, components of hemorrhage at various stages, cellular infiltration, deposition of short T2 tissues (eg, amyloid), iron deposition, deposition of other paramagnetics, malignant melanoma, thrombosis clots and emboli, cryoablation, and administration of magnetic iron oxide particles (MIOPs). These processes may increase the concentration of the short T2 components by the addition of new tissue with a short T2 as well as by shortening the T2s of the long T2 components in tissue. The signal from short T2 components may also be increased by shortening their T1.

There are also many processes that may decrease the signal from short T2 components. These include many of the diseases that typically increase tissue T1s and T2s such as edema, acute inflammation, infection, infarction, and many tumors. Loss of order in a highly structured tissue such as collagen may also lead to a decrease in signal from its short T2 components. Reduction in signal from T2 components may also result from a decrease in their concentration, a decrease in their T2 into the extremely short T2 range, and an increase in their T1.

BASIC PHYSICS

This section outlines features of the MR physics, which particularly apply to UTE imaging. The most important general concept is that during any rf pulse, there is competition between the pulse tending to rotate the magnetization into the transverse plane and relaxation processes tending to decrease magnetization in the transverse plane. With long T2 species such as free water, relaxation during the rf pulse is minimal, and the magnetization of the protons is fully rotated through the specified flip angle (eg, 90°) into the transverse plane. However, with short T2 species, where T2 is of the same magnitude as the duration of the rf pulse or shorter, relaxation processes dominate and the magnetization actually rotated into the transverse plane may be very much less than that expected from the nominal pulse flip angle (Fig. 4). At the same time the longitudinal magnetization is partly saturated so that overall, there is a reduction of magnetization in the transverse plane with a decrease in the longitudinal direction. In sequences designed for imaging of short T2 species, it is therefore necessary to use short rf excitation pulses. This also means that the effective duration of an rf pulse is loaded toward its later stages for short T2 species because these may relax significantly during the earlier stages of the pulse.

This situation may be exploited by purposely using pulses of long duration to rotate selectively long T2 components into the transverse plane but leave short T2 components largely unaffected. For example, to reduce the signal from long T2 components, a long duration (eg, 10 milliseconds) rectangular 90° pulse may be used to rotate the long T2 components into the transverse plane and then dephase them with crusher

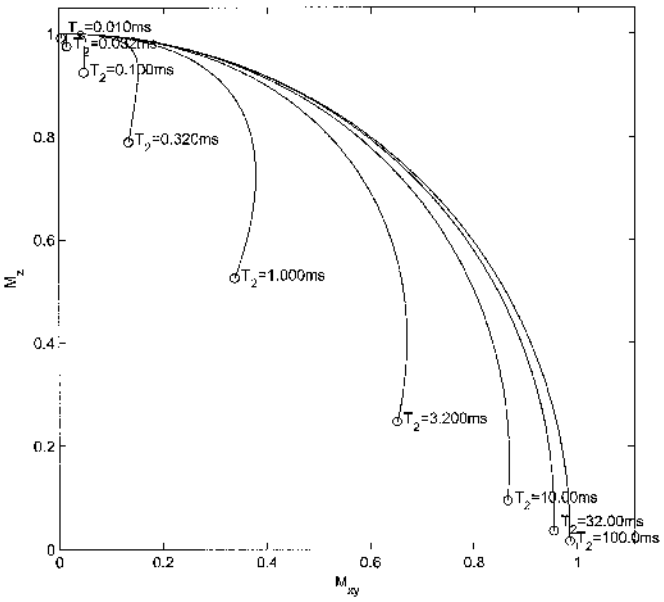

FIGURE 4. Simulation of the magnetization trajectory during a 3-millisecond, 90° rectangular pulse showing rotation of longitudinal magnetization (M_z) into the transverse plane to become M_{xy} for tissue T2s between 0.01 and 100 milliseconds. For a tissue with T2 = 100 milliseconds, rotation is almost complete, but as T2 is decreased, less magnetization is rotated until, for T2 = 0.01 milliseconds, there is virtually no magnetization rotated into the transverse plane. Changes to M_z are also reduced with decreasing T2.

gradients while leaving the short T2 components largely unaffected.[22]

These considerations not only apply to 90° and lower flip angle pulses, but also to inversion pulses. These are of necessity longer than 90° pulses and longer again if they are slice selected. Depending on the duration of the pulse, a short T2 tissue may be unaffected, partially saturated, or saturated or partially inverted by such a pulse (Fig. 5).

While it can be very difficult to invert short T2 components, it is much easier to saturate them. To do this they need to be excited, but the dephasing process is then very effective and very short T2 components may not even need a subsequent dephasing gradient pulse. As a result, methods of measuring T1s of short T2 components that include inversion pulses are fraught with difficulty while those utilizing saturation pulses are relatively straightforward.

Another basic difference from conventional MR is the fact that short T2 components have broad line-widths and therefore may be saturated by off-resonance rf pulses (Fig. 6). This may arise in a number of ways. The use of fat suppression techniques with pulses 220–230 Hz off-resonance (at 1.5 T), which are relatively close to the resonant frequency may partially saturate the broad lines of short T2 components and thus reduce the signal available from them. Decreases of 10% to 20% in available signal from this source can readily be demonstrated.

The use of multislice and multiecho imaging where slices are selected in different locations by use of different resonance frequency offsets is another situation where reduction in signal from partial saturation of broad line components can be demonstrated. These effects are in addition to the deliberate application of off-resonance pulses with magnetization transfer (eg, 1500 Hz off-resonance at 1.5 T) which also saturate and thus reduce the signal available from short T2 tissues.

There are other differences from conventional imaging. The rapid decay of the signal from short T2 components means that the time available for useful sampling of them is much less than that for long T2 components that do not decay significantly during a typical data acquisition of 10–20 milliseconds duration. The decay of signal during the data acquisition can result in the loss of high-resolution detail because the amplitude of the signal may be low or zero when the outer regions of k-space are mapped (Fig. 7).

The distinction between T2 and T2* is significant in this context. T2 is the spin-spin relaxation time and is a fundamental property of tissue (at a specific field strength, temperature, and so forth). It is usually measured with a Carr-Purcell-Meiboom-Gill sequence with a series of phase-alternated inversion pulses, which, within fairly broad limits, gives values of T2 largely independent of the measurement technique. On the other hand, T2* is the relaxation time observed with a gradient echo pulse sequence and includes both T2 relaxation and

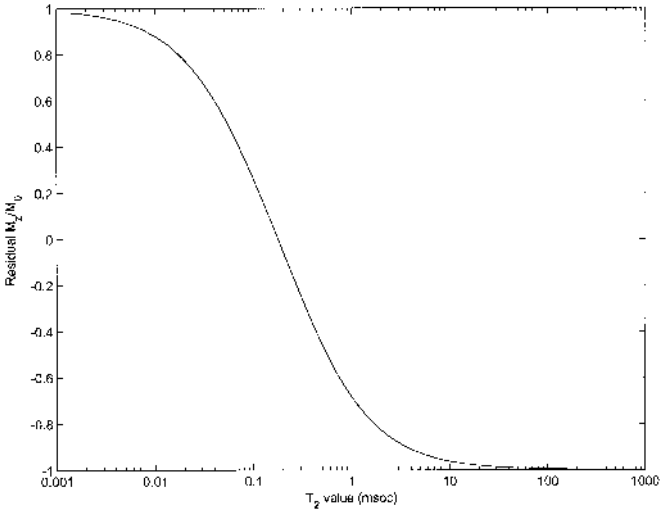

FIGURE 5. Effect of a short inversion pulse (0.50 milliseconds) on magnetization (M_z) for tissues with different values of T2. The residual magnetization, M_z/M_o, present after application of the pulse is plotted against T2. With T2s of 100 milliseconds or more, the magnetization is almost fully inverted (ie, $M_z/M_o = -1$), but with short T2s (eg, 0.01 milliseconds), very little magnetization is inverted.

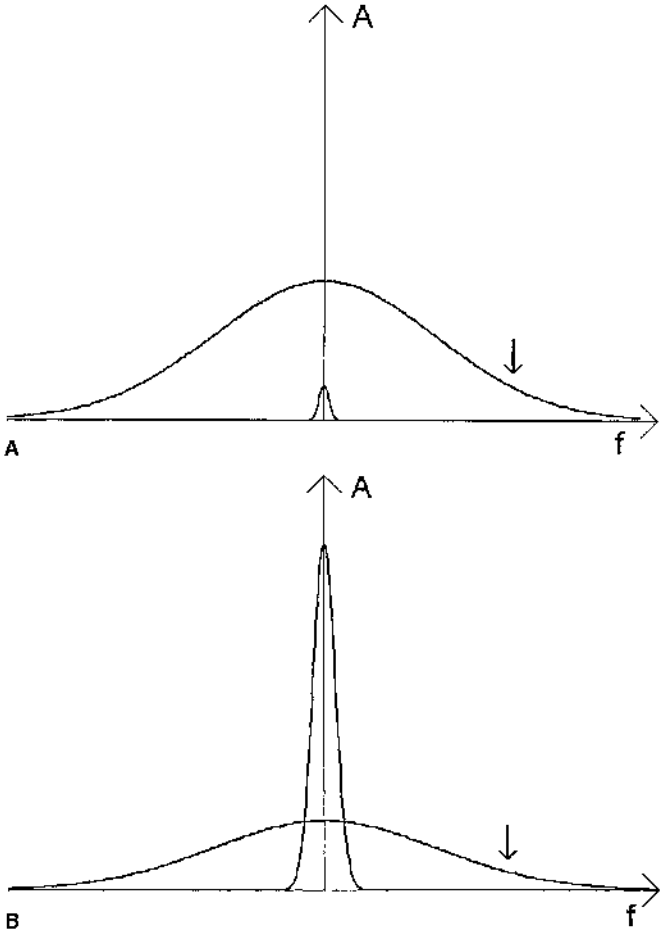

FIGURE 6. Stylized spectrum of (A) a tissue with a majority of short T2 components and (B) one with a minority of short T2 components. Amplitude (A) is plotted against frequency (f). The short T2 components have a broad line while the long T2 components have a narrow line. The off-resonance pulse in (A) (arrow) saturates the broad line and reduces the signal that can be detected from these components with a UTE sequence. The off-resonance pulse in (B) (arrow) saturates the broad line, which then exchanges with the larger narrow line (long T2) pool and produces a reduction in the magnetization detected from it with conventional TE sequences. With UTE sequences, both the direct saturation of the short T2 components and the indirect effect on the long T2 components via magnetization transfer are detectable.

coherent dephasing effects which are highly dependent on the imaging technique used. These dephasing effects arise from spins within a voxel which have different precessional frequencies. The difference in frequency is affected by voxel dimensions including slice thickness. In general the larger the voxel, the greater the field inhomogeneity within it and the greater the dephasing effect. Specification of T2* thus requires a knowledge of voxel size and field inhomogeneity within it.

The difference between T2 and T2* may be greatly reduced if TE is decreased from conventional values of 10 milliseconds to 0.1 milliseconds or less. Dephasing effects due to causes such as poor shimming or inhomogeneity in large voxels at air-tissue interfaces are reduced.

In a given tissue we may not be able to say conclusively that we are observing a T2 change and not a T2* change when imaging with a gradient echo type of sequence without additional information. In tissues that are known to contain no dephasing sources, it is reasonable to assume that the measurement essentially reflects T2 while in other tissues (eg, cortical bone) we need to be more cautious as dephasing effects may be affecting the signal even at ultrashort TEs.

The one technique in clinical MR imaging that has previously provided access to the otherwise undetectable short T2 components in tissue is magnetization transfer. By applying

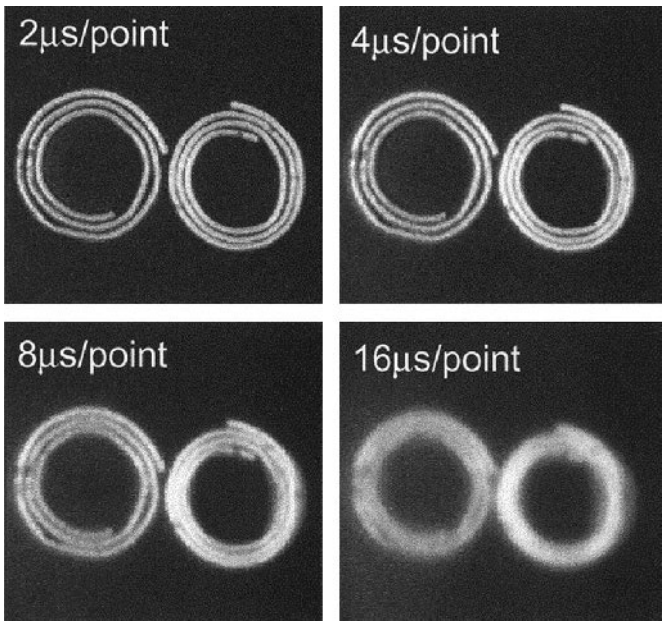

FIGURE 7. CUTE (TR/TE = 200/0.07 milliseconds) images of two 2-mm-thick rubber straps (T2 = 0.8 milliseconds) wrapped concentrically around 0.5-mm (right) and 1-mm (left) cardboard spacers. The straps give a detectable signal, but the spacers do not. Images were acquired with 210-mm FOV, which should yield 0.4-mm spatial resolution. Rapid data acquisition (2 microseconds/point giving a 1-millisecond data collection) resolves the boundaries of the straps accurately (top left). With 4 microseconds/point sampling giving a data collection of 2-milliseconds duration, there is some slight blurring (top right). With 8 microseconds/point and a data collection of 4 milliseconds, blurring becomes obvious (bottom left) and with 16 microseconds/point and 8-milliseconds data collection, blurring is so marked that the internal boundaries are hardly resolved at all. The loss of definition is due to the rapid decay of the signal from the rubber straps during the data collection. This is minimal when the acquisition is of 1-millisecond duration and thus only slightly greater than the T2 of the straps (0.8 milliseconds), but is obvious when the acquisition is of 8-milliseconds duration and thus 10 times longer than the T2 of the straps.

off-resonance rf pulses it is possible to saturate the short T2 (broad line) components while leaving the long T2 (narrow line) components unaffected and to detect the effect of this saturation through the exchange that occurs between the otherwise undetectable short T2 components and the detectable long T2 components which are imaged. This indirect technique for imaging of short T2 components has advantages over conventional techniques in applications such as detecting abnormalities in normal-appearing white matter. The technique is applicable to tissues with a minority of short T2 components (because they also have long T2 components that provide the detectable signal) and to tissues where the short and long T2 components are in exchange. Magnetization transfer can provide indirect access to very short T2 components (eg, with T2s of 1–10 microseconds) that are not directly detectable with UTE imaging.

MACHINE PERFORMANCE

To put clinical MR system performances in context for this type of study, it is worth noting the performance of imaging spectrometers used for solid-state studies on small samples (milligrams or grams) with very short T2s. Typically these systems utilize short rf pulses (eg, 1–2 microseconds duration) with high peak power, a broad bandwidth and rectangular pulse profiles. The spectrometer can switch very rapidly from transmit to receive mode (eg, in 1 microsecond or less) so signal loss due to the rapid decay of short T2 components is minimized. Available gradient strengths (over a very small field of view) are much higher and rise times much shorter than those on clinical systems. In addition, B_os are usually higher providing a greater signal-to-noise ratio. Biological safety issues are not a concern with inanimate samples.

In comparison, when examining humans (kilograms) on clinical MR systems, transmitter coils are large, and B_1 power limitations means that the shortest rf pulses are of the order 0.25–0.40 milliseconds in duration, depending on flip angle. This value is similar to that of the T2 of tissues such as cortical bone as well as that of the short T2 components in other tissues.

With present-day clinical MR systems that are used primarily to image long T2 components, there has been no particular demand for rapid switching from transmit to receive mode, so typical minimum switching times are of the order 0.08–0.10 milliseconds. This allows time for highly resonant transmitter coils to ring down, but it may lead to loss of a significant proportion of the signal from short T2 components.

Gradient performance, first to ramp the gradients up and then to maintain them at a high amplitude, is of importance when imaging tissues or tissue components with short T2s. As a general rule, the duration of useful data collection for a short T2 component is of the order T2 or twice T2. If gradient performance is limited both in slew rate and maximum strength, a significant proportion of the short T2 signal may be lost before it can be spatially encoded.

ULTRASHORT TE PULSE SEQUENCES

With conventional 2DFT imaging, there is a delay after the initial rf excitation when the slice selection gradient is used to rephase the signal. Time is also required for the phase encoding pulses, the initial dephasing lobe of the frequency encoding pulse, and the first half of the data acquisition before the center of k-space is reached. The term "2DFT" is used to describe rectilinear sample of k-space. It is also known as phase-frequency encoding or spin-warp imaging although both this method and UTE sequences use 2D Fourier transforms to reconstruct the image (after the data has been regridded in the case of UTE imaging).

It is possible to avoid the need for rephasing of the slice-selective rf excitation pulse by first collecting the data with the slice selection gradient in one direction and adding this to data collected in the same way with the slice selection gradient reversed (Figs. 8–10). At the end of this process, the signal is effectively in-phase and data sampling can, in principle, begin as soon as the rf pulse and the slice selection gradient are ramped down to zero. The use of radial imaging of k-space with the acquisition starting in the center of k-space (where no gradient is required for the initial encoding) means that there is no need for a phase-encoding gradient, a read-dephasing gradient, or additional time to get back to the center of k-space in the read direction. Data sampling can continue while the gradient is being ramped up (although sampling during ramping takes a longer time than when the gradient is fully ramped up

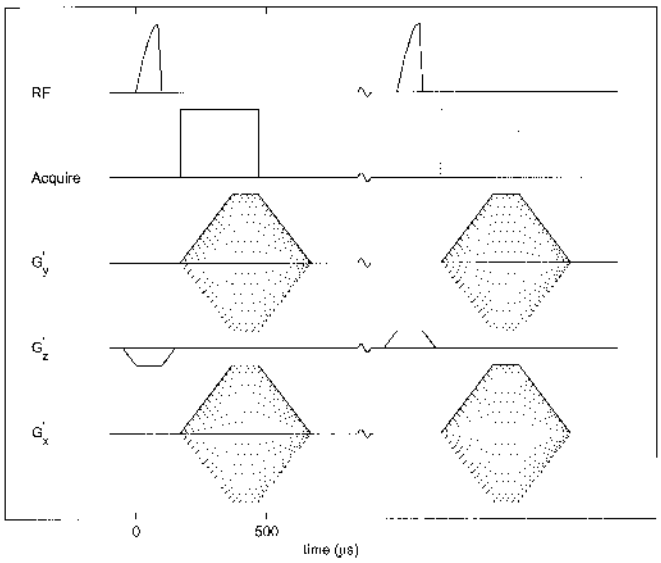

FIGURE 8. Pulse sequence diagram for a basic UTE sequence. The half rf pulses are applied with the slice-selection gradient G'_z negative in the first half and with this gradient positive in the second half. The rf pulse is truncated and followed rapidly by the acquisition during which G'_x and G'_y are applied to give the radial gradient. These gradients ramp up to a plateau during data acquisition.

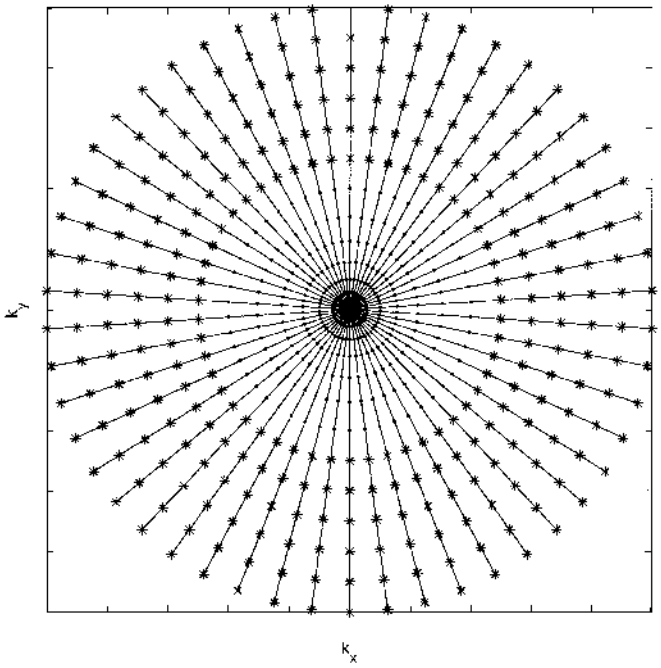

FIGURE 9. k-space trajectories for the above imaging sequence. Each "spoke" represents the k-space trajectory due to the readout gradients. The dots represent the central points that are sampled on the gradient ramps and the stars the peripheral points that are sampled on the gradient plateau. Practical acquisitions typically include 128–512 spokes and 256–512 points on each spoke. The data points are regridded onto a Cartesian grid prior to 2D Fourier transformation.

by a factor of about two) as well as after the gradient has reached its plateau. The gradient also needs to be ramped down very quickly at the end of the rf excitation because persistence of the gradient after the end of the rf pulse may result in dephasing of the signal.

It is usual to take TE as the time from the midpoint of the rf excitation pulse to that of the sampling of the center point of k-space. This is appropriate (or only slightly in error) for long T2 components, but the precise value of TE may become uncertain with short T2 components. The effectiveness of the rf pulse is biased toward the end of excitation for short T2 components so the endpoint of the rf excitation may be more appropriate to use as the time origin for TE.

The pulse sequence is not a spin echo or gradient recalled echo (because reversed gradients are not used to form an echo). There is no echo because the signal is not refocused and each half excitation is not fully rephased. It is only after they are added that the k-space data is in phase. Echoes are formed with most types of clinical imaging and for simplicity it is usual to regard the UTE sequence as a type of gradient echo.

While simple UTE sequences are effective for imaging tissues with a majority of short T2 components, some form of long T2 component reduction is necessary to selectively image short T2 components in tissues in which they are a minority [Fig. 11(A)]. The initial approach to this problem was to use a long (eg, 10 milliseconds) rectangular 90° pulse followed by a dephasing gradient as explained above. Another method involves the use of an initial long inversion preparation pulse (eg, 4 milliseconds) to selectively invert long T2 components followed by a time inversion (TI) chosen to null them. This technique requires knowledge of the T1 of the long T2 components. Comparison with the same procedure but making use of a short inversion pulse (eg, 0.40 milliseconds) in an attempt to invert simultaneously both long and short components provides a measure of the effectiveness of the technique. A third method is to subtract a later echo image from the first (UTE) one and produce a difference image [Fig. 11(B)]. Tissues or fluids with a long T2 have their signal attenuated by this procedure while tissues that have a short T2 and decay rapidly between the two echoes are highlighted on the resulting difference image.

Pulse sequences employing half rf pulses and radial sampling were first implemented for clinical purposes by Bergin et al from Stanford in 1991 and 1992[4,5] and were initially applied to lung imaging. This implementation incorporated spectroscopic imaging and a modified Dixon technique for separation of fat and water signals as well as a 90° rectangular preparation pulse for suppression of long T2 components. We have implemented half rf excitations with center-out radial mapping of

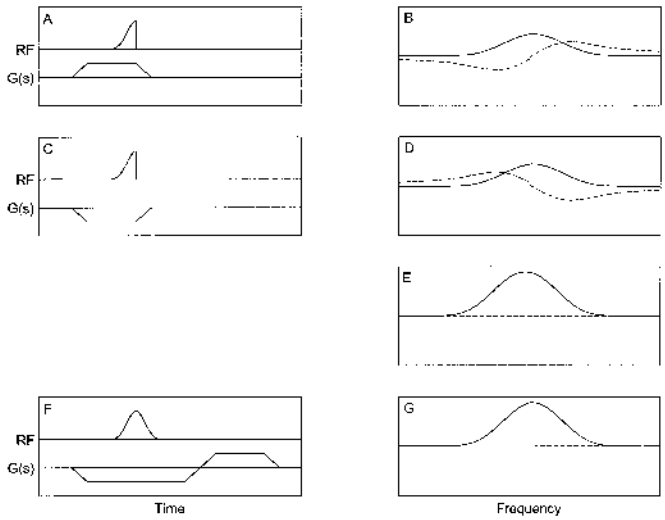

FIGURE 10. Slice profiles with UTE sequences. The two half-pulse excitations are shown in (A) and (C). The slice profile from these acquisitions are shown in (B) and (D), respectively. The continuous line is the real component, and the dotted line is the imaginary component. The slice profile from each half acquisition is broad. If the data in (B) and (C) are added in the complex domain, a narrow profile is obtained as shown in (E). Conventional sequence slice selection (F) produces the profile shown in (G) which is the same as (E). The need for short rf pulses predicates against a sharp-edged slice profile.

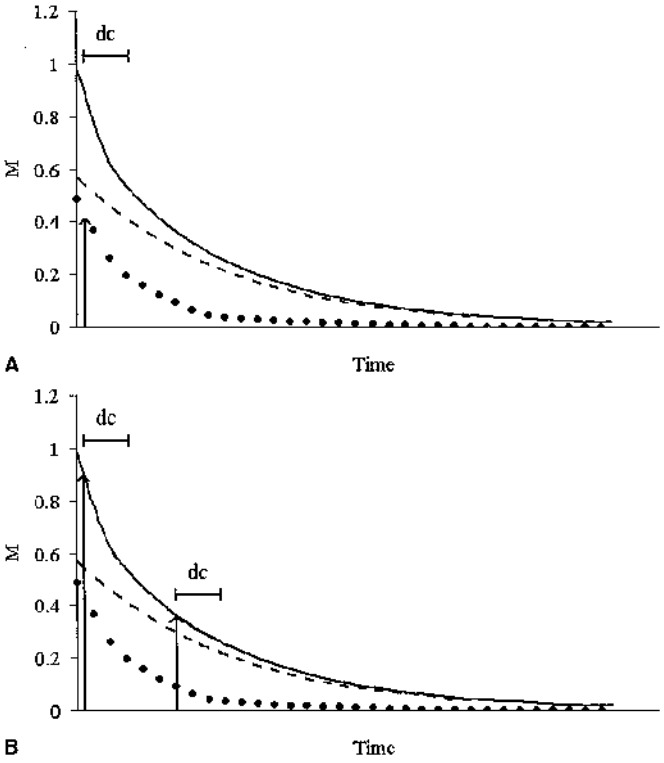

FIGURE 11. Long T2 reduction techniques using either a long T2 (90°) suppression pulse or long inversion pulse nulling are shown in (A) and subtraction of a later echo from an earlier one in (B). The total magnetization is shown as a continuous line, the short T2 components as circles, and the long T2 components as dashes. Reduction of the long T2 components in (A) reduces the detectable magnetization to that from the short T2 components (vertical arrow). In (B), subtraction of the second echo from the first produces a difference image in which most of the signal comes from the short T2 components because they decay rapidly between the two echoes.

k-space with TEs of 0.07 or 0.08 milliseconds but in a more modular form, details of which are given below.

Truncated rf pulses of 0.40–0.50 milliseconds duration are used with slice-selective gradients applied in one direction and then reversed for the second half of the acquisition. The two sets of data are added to give a single radial line of k-space, and the process is repeated through 360° in 128–512 steps. The data is mapped onto a 512 × 512 grid and reconstructed by 2D Fourier transformation to give a gradient echo type of image. Four sets of images with typical TEs of 0.08, 2.87, 5.66, and 8.45 milliseconds [at 2 microseconds per analogue to digital converter (ADC) sample] or 0.08, 5.95, 11.08, and 17.70 milliseconds (at 4 microseconds per ADC sample) are usually obtained. The length of the ADC sample point during the acquisition represents a compromise between (at 2 microseconds) acquiring data before the signal had significantly decayed (but at a wide bandwidth that decreases signal to noise ratio) and (at 4 microseconds) acquiring data for longer, which allows the signal to decay further (but with a narrower bandwidth and hence increased signal-to-noise ratio). Data is usually sampled over 256–512 points. Slice selection in multislice sets is performed with sequential excitations with the positive gradient followed by sequential excitations with the negative gradient. Contiguous multislice interleaved excitations may interfere directly with the half rf pulse because the slice profile of a half pulse alone is spread out. Versions of the basic sequence with frequency-based fat suppression and/or long T2 component suppression have been implemented. Initial short (0.40 milliseconds) and long (4 milliseconds) inversion pulses are used as preparation pulses. With each variant of the sequence, difference images formed by subtraction of subsequent echo images from the first echo image are produced. The abbreviations used to describe these sequences are listed in Table 4. Fields of view of 12–40 cm are employed with slice thicknesses of 4–8 mm. Two to 20 multiple interleaved slices are obtained. TRs of 500 milliseconds are commonly used with conventional ultrashort TE (CUTE) and fat-suppressed ultrashort TE (FUTE) sequences with flip angles (for long T2 components) of 45° to 80° and slice gaps of 10% to 100%. Serial studies of contrast uptake use a TR of 50–100 milliseconds. Inversion recovery sequences had TRs of 650–2500 milliseconds. Breath-hold and cardiac gated sequences use TRs of 10 milliseconds. Scan time varied from 12.8 seconds to 17 minutes. All studies were performed on Sonata 1.5-T systems (Siemens, Erlangen, Germany).

To measure T1 values in short T2 species (eg, for cortical bone) a saturation pulse was used with a series of saturation recovery delays (TSR) prior to excitation and acquisition. Analysis involved the placement of regions of interest within the tissues, subtraction of the signal from long T2 components, and fitting of the resulting intensity versus TSR curves to a saturation recovery model.

To measure T2* values (eg, for cortical bone), TEs for the first echo of 0.14, 0.30, 0.46, 0.78, 1.10, 1.52, 1.94, and 2.46 milliseconds were used with a TR of 500 milliseconds. Images with the shortest available TE (eg, 0.07 milliseconds)

TABLE 4. Acronyms for Ultrashort TE Pulse Sequences

UTE	Ultrashort TE
CUTE	Conventional ultrashort TE
FUTE	Fat-suppressed ultrashort TE
LUTE	Long T2-suppressed ultrashort TE
FLUTE	Fat and long T2-suppressed ultrashort TE
STUTE	Short TI inversion time ultrashort TE
MUTE	Medium TI inversion time ultrashort TE

d = difference image produced by subtraction of a subsequent image from the first. l = long, s = short inversion pulses (used with STUTE and MUTE sequences). Breath-hold, cardiac gated, and double-inversion recovery forms have been implemented.

were not acquired owing to the existence of small eddy-current effects from the slice-selection gradients. Analysis involved placement of regions of interest and fitting the resulting intensity versus TE curves to an exponential decay with an offset (due to the presence of small concentrations of long T2 components).

To summarize, the key features of UTE sequences are listed below.

1. Preparation pulses: With UTE sequences, these are similar to conventional pulses, but inversion pulses may only affect long T2 components. Long inversion pulses can be used for nulling of these T2 components. Magnetization transfer pulses may directly saturate short T2 components and diminish their signal. Fat saturation and multiple slice multiple echo imaging may do the same.
2. Rf excitation and slice selection. This must be short and ideally less than the T2 of the components of interest. The rf pulse is truncated. Slice selection is achieved in two halves with reversed gradients to avoid the need for a rephasing gradient lobe.
3. Data acquisition can begin as soon as each half of the slice selection is completed and rf switching allows.
4. Mapping of k-space: Radial mapping from the center of k-space is performed (without phase encoding pulses) including acquisition during the ramping up of the gradient. This should be completed in a time of the order of the T2 of the tissue of interest. Data acquisition is at wide bandwidth.
5. Image reconstruction: The radial data are regridded into rectangular coordinates and are reconstructed using 2DFT.
6. Postacquisition: Subtraction of later echoes from the first is useful for selectively reducing the signal from long T2 components.

CONTRAST ENHANCEMENT

Intravenous gadolinium chelates (eg, gadodiamide 0.3 mmol/kg) may show enhancement in tissues with short T2s using UTE sequences when this is not apparent with conventional sequences because no signal is detectable from them either before or after contrast administration. The effect results from a shortening of T1 and may be of particular interest because some tissues with a majority of short T2 components are avascular or relatively avascular, and contrast enhancement may allow solute transport or perfusion to be studied within them. The detection of normal enhancement in tissues with short T2s may allow a reduction in this enhancement to be recognized in disease (see Fig. 19). Even in tissues where signals are detectable with conventional sequences, the signals from the majority of longer T2 tissues may be detected earlier during their decay, and signal from the minority of short T2 components may also be detected. This may allow the tissue to be visualized with a higher signal intensity before enhancement and to show a greater increase in signal after enhancement (see Fig. 17).

Another feature of interest with UTE sequences is that they may be able to detect signals from tissues with short T2s and concurrently reduce or suppress signals from tissues or fluids with long T2s. This can be achieved by the use of different long T2 reduction techniques. This option may be useful with contrast enhancement with gadolinium chelates where frequently the greatest change is seen in blood (which has a long T2), but the area of most clinical interest may be adjacent or associated tissue with a short T2 (see Fig. 15).

Magnetic iron oxide particles (MIOPs) typically produce a loss of signal through susceptibility effects. This loss of signal may not be manifest with conventional sequences in tissues that produce no signal prior to enhancement such as tendons and ligaments. In this situation, the presence of these particles may be inferred by loss of signal in surrounding tissues or fluids which have detectable MR signals. The use of UTE sequences to produce a detectable signal in the tissues of interest may provide a baseline to recognize a reduction in this signal produced by MIOPs.

A particular problem with intravenous use of MIOPs is that they frequently produce a loss of signal in the area of most interest, which may make image interpretation difficult. (Gadolinium chelates as most commonly used clinically do the reverse by increasing the signal in the area of most interest.) Also, with the use of oral MIOPs to reduce the unwanted signal from bowel contents, the loss of signal may extend beyond bowel and produce loss of signal in adjacent organs. UTE images typically show low sensitivity to susceptibility effects, but later echo images show higher sensitivity to these effects. Subtraction of a subsequent echo from the first produces a difference image in which the anatomic detail from the first (UTE) image is well preserved, but modulated by the susceptibility dependent contrast developed by the later echo, with higher signal on the difference image representing a greater degree of susceptibility effect.

IMAGE INTERPRETATION

The interpretation of UTE images follows established principles, but there are some interesting differences. The term "T2-weighted" as usually applied to a pulse sequence is generally taken to mean weighting for long T2 components in a tissue or fluid by use of a long TR and long TE. Sequences may also be T2-weighted, but for short T2 components (ie, with T2s less than 10 milliseconds) using short TEs rather than long ones. For clarity, in situations where there may be confusion, it may be necessary to use the terms "long T2-weighted" and "short T2-weighted." Sequences may be both short T2- and T1-weighted at the same time if they have a short TE and a short TR or just short T2-weighted if they have a short TE and long TR (relative to T1).

As a rule, the T2 weighting of a sequence is maximal for small increases or decreases in the T2 of a tissue when its TE is about the same as the tissue T2. Thus UTE sequences alone

(eg, TE = 0.08 milliseconds) are not particularly T2-weighted for most tissues in the short T2 range because these tissues often have longer T2s. Although the T2 weighting of UTE sequences is low for most short T2 tissues, T2 weighting increases for tissues in the short T2 range with later echoes (eg, with TE = 2.87, 5.66, and 8.45 milliseconds). These may detect an increase or decrease in signal intensity in disease relative to normal tissue.

The long T2 reduction techniques also effect T2 weighting, but in a different way. They selectively attenuate the signal from tissues with long T2s leaving only the short T2 components. As a result, the sequence only shows signal from tissues with T2s within a restricted range or window (Fig. 12). Tissues may enter or leave this window of visibility at either end by increasing or decreasing their T2s. The width of the window varies with the duration of the rectangular pulse, the length of the nulling inversion pulse, or the TE of the subtracted echo. Within the window, the above consideration about the choice of TE in relation to T2 apply. The situation may be complicated by tissues having two or more components in the short T2 range present in significant concentrations.

UTE sequences are T1-weighted if the TR for CUTE, FUTE, long T2-suppressed ultrashort TE (LUTE), and fat and long T2-suppressed ultrashort TE (FLUTE) sequences is about the T1 of the tissue of interest, with due allowance for flip angle. This is the common situation. With inversion recovery sequences, T1 weighting is maximal if the TI is about the T1 of interest. Cortical bone has a T1 in young and middle-aged subjects of 130–160 milliseconds at 1.5 T which is shorter than subcutaneous fat. The T1 of cortical bone increases significantly with age to 260–280 milliseconds in the ninth decade. Tendons, ligaments, and menisci have relatively short T1s in the range 300–600 milliseconds at 1.5 T. T1s of short T2 components in tissues in which they are in a minority are less well characterized, but are probably similar.

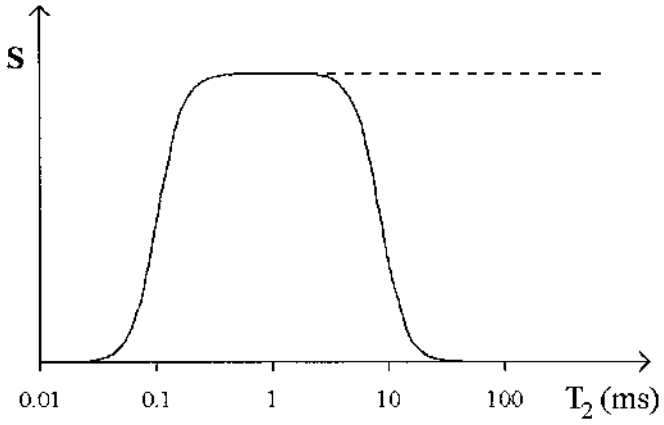

FIGURE 12. Stylized sensitivity profile of a UTE sequence to tissues with different T2s shown on a logarithmic scale. The lower cut-off point is set by machine performance and is probably between 0.01 and 0.1 milliseconds. Without T2 reduction, the sequence is sensitive to T2 components in the range 1–10 milliseconds and higher (dashed line). With T2 reduction techniques, the sensitivity to longer T2s is reduced to zero (continuous line). There is thus a window of short T2s to which UTE sequences with long T2 reduction techniques are sensitive. Tissues can enter or leave this window of visibility by increasing or decreasing their T2s. (The graph does not take into account differences in concentration of T2 species or the effects of T1 which both affect the detectable signal.)

Conventional proton density weighted pulse sequences with typical TRs of 2000–3000 milliseconds and TEs of 10–20 milliseconds do not detect a number of short T2 components that contribute to proton density as measured by chemical assay. Even UTE sequences do not detect extremely short T2 components. However, changes in proton density may be a greater source of contrast when imaging with short T2 components than is the case with long T2 components.

With inversion recovery sequences, the use of a long initial inversion pulse may mean that long T2 components may experience an inversion recovery sequence while short T2 components experience a partial saturation type of sequence because they do not experience the inversion pulse. Thus, with long TRs, short T2 components may fully be recovered while long T2 components may still be recovering their longitudinal magnetization after the inversion pulse.

Each of the long T2 reduction techniques has advantages and disadvantages. Long T2 component suppression with a long preceding 90° pulse and dephasing has the disadvantage that no unsuppressed image is available, but the advantage that susceptibility effects are not introduced by subtraction of a later echo. However, susceptibility effects may render the long narrow bandwidth pulse ineffective and result in high-unsuppressed signal from long T2 components. The long inversion pulse sequences with nulling of long T1 components may be difficult to interpret due to magnitude processing and concerns about whether the chosen TI is correct. Subtraction images increase the noise level and introduce susceptibility effects, but both the original images and the subtracted image are available for examination.

With LUTE, FLUTE, and l STUTE sequences, comparison of the first and subsequent echo signal intensities using difference images provides a measure of the success of the long T2 reduction technique. If there is considerable reduction of signal between the two echoes, then what is being imaged is mainly short T2 components.

Changes induced by susceptibility effects may be obvious on later echo images and may not require subtraction from the first UTE to make them obvious if they are seen against a uniform tissue background. Subtraction may be more useful at interfaces and other regions where there is complex anatomy (eg, with meninges and blood vessel walls) or where it may be desired to visualize short T2 components without confounding

effects from tissues or fluids with long T2s such as contrast-enhanced blood.

To selectively show short T2 components, subtraction images must have adequate signal-to-noise ratio. Thus, cortical bone may be obvious in a subtraction image when it is situated close to a surface coil, but be of low signal on all sequences (including subtraction images) when examined at some distance away from the conductors of a body coil.

When double inversion recovery pulses ("black blood pulses") are used to reduce the signal from blood, the two inversion pulses may saturate the signal from short T2 components in vessel walls.

Magic angle effects in tendons and ligaments are manifest as a relative increase in signal on later echo images (due to the longer T2) and a decrease in signal on difference images. These can be seen in the anterior cruciate ligament (ACL), on the femoral side of the posterior cruciate ligament (PCL), as well as at other sites.

The conspicuity of increased or decreased signal from short T2 components within a tissue differs depending on whether these components are in a tissue with a majority of short T2 components or in a tissue with a minority of short T2 components where the effect may be diluted unless the signal from long T2 component is reduced. Likewise, the effect of a T2 shortening process may be more obvious in a tissue with a minority of short T2 components than in one with a majority where there are no long T2 components available in the tissue to have their T2 reduced.

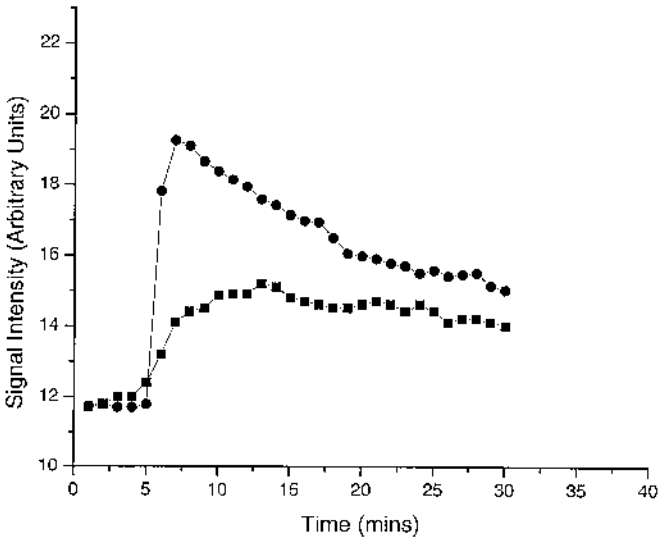

FIGURE 13. Signal intensities in cortical bone after fracture of the tibia. Intravenous gadodiamide was given after 5 minutes. Results in 1 patient 4 days after fracture (squares) are compared with those in another 3½ months after fracture (circles). There is a faster and higher increase in signal in the patient imaged 3½ months after his fracture.

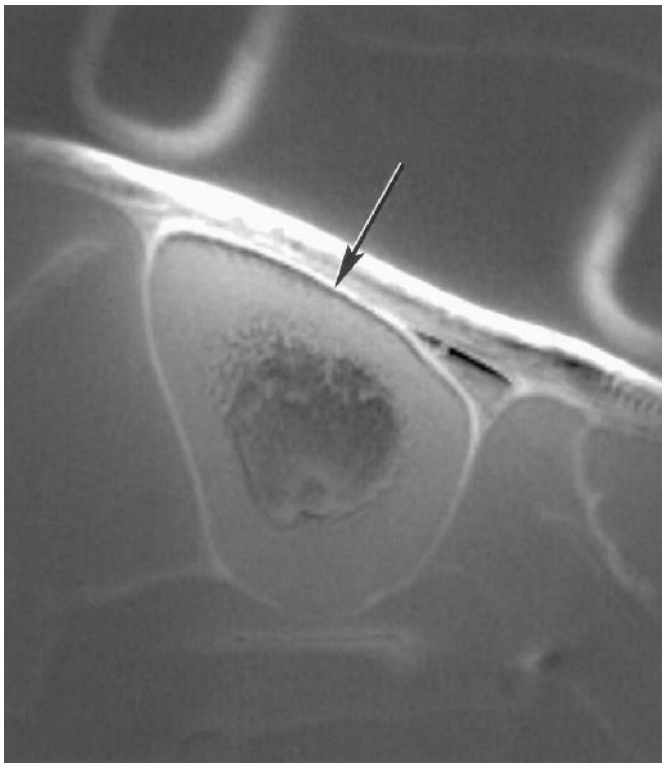

FIGURE 14. Normal tibia. Transverse d FUTE (TR/TE = 500/0.08 minus 5.95 milliseconds) image. The periosteum (arrow) is highlighted.

Even when it is not necessary to reduce the signal from long T2 components in a tissue of interest with a majority of short T2 components to visualize them (eg, tendons, ligaments), it may still be useful to do this to increase the conspicuity of these tissues by reducing the signal from other tissues with a minority of short T2 components.

Diseases that increase the T2 of tissues with a majority of short T2 components may render them more obvious on later echo images, but less obvious on difference images (ie, the increase in T2 takes them outside the visible window in Fig. 12). With conventional pulse sequences, contrast enhancement in these tissues (eg, tendons and ligaments) may only be recognizable in areas where the T2 is increased so that signal is detectable. Paradoxically, with difference images, these may be just the areas where contrast enhancement is not visible on difference images because the increased T2 leads to attenuation of the signal.

Tissues with long T2s but short T2*s are common at tissue-air interfaces. Susceptibility effects affecting the mucosa of the nasal sinuses are obvious with later echoes and on difference images. Fatty bone marrow within trabecular bone contain significant short T2* components. Large bowel contents typically have a short T2 and/or T2* and display a high signal on UTE and difference images derived from them. The

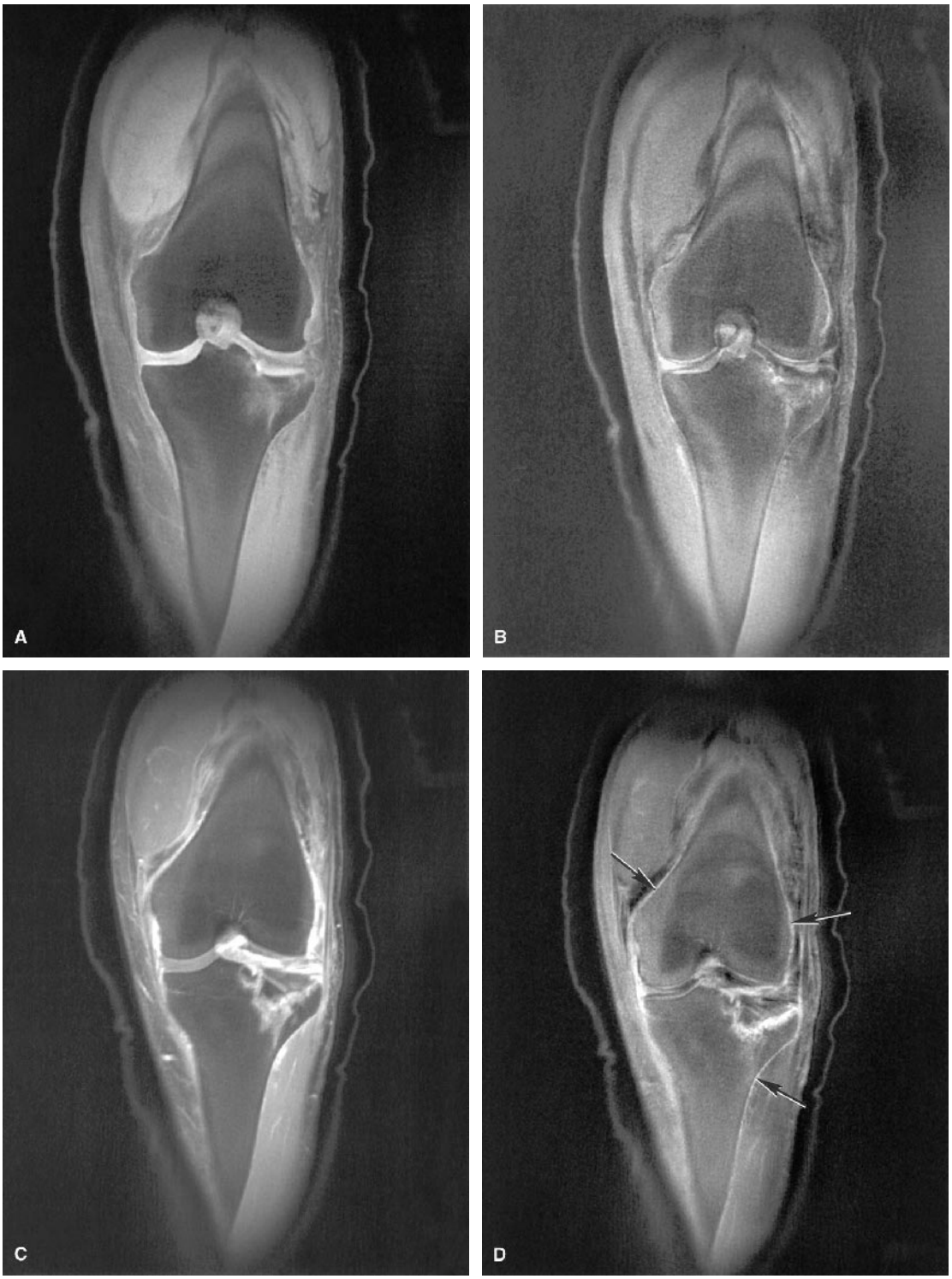

FIGURE 15. Fracture of the tibial plateau 3 days after injury. (A) Coronal FUTE (TR/TE = 500/0.08 milliseconds) and (B) d FUTE (TR/TE = 500/0.08 minus 5.95 milliseconds) images before enhancement and the same (C) FUTE and (D) d FUTE images after enhancement. The periosteum is just seen in (B). Marked enhancement of blood vessels and other tissues is seen in (C), but subtraction specifically shows the enhanced periosteum in (D) (arrows).

FIGURE 16. Sagittal d FUTE (TR/TE = 500/0.08 minus 11.08 milliseconds) image of the posterior cruciate ligament (PCL) (A) before and (B) after enhancement. A focal area of enhancement is seen on the tibial side of the ligament (arrow).

signal at the lung bases on subtraction images seen in normal volunteers probably represents a short T2* effect due to susceptibility effects either from fluid in lung or blood. Lung has short T2 components as well as short T2* components.[14]

Particular artifacts associated with the use of UTE sequences include radial lines, susceptibility effects, out-of-slice effects, flow dephasing effects, and effects due to delayed rf switching. Radial artifacts resemble those seen with CT. Susceptibility artifacts may be manifest as high signal on difference images. However, within cortical bone they may produce a relative increase in signal on late echo images and have a low signal (rather than a high signal) within the bone on difference images. Out-of-slice artifacts can produce high signal at boundaries or interfaces. Materials with short T2s in the receiver coils often have a high signal. Plastic intrauterine contraceptive devices (IUCDs) also have a high signal as do various items of clothing. Bone may be diamagnetic to a different degree than other tissues, and this may result in phase cancellation at boundaries. Large artifactual changes on difference images can arise from subtraction of later out-of-phase (fat and water protons) echo images from the first (UTE) image. Motion artifact is more prominent with later echoes and becomes more obvious on difference images. Flow of blood can lead to dephasing on the later echo images and a high signal on difference images, which simulates signal from short T2 components. Delay in coil switching and/or eddy currents may produce a mottled effect, and a relative reduction of the first echo compared with the second, with negative signals on difference images.

CLINICAL ILLUSTRATIONS

To date, we have studied over 120 patients using the techniques described above. The selection of patient groups follows from a number of considerations. The detection of signal from tissues with short T2s, which have previously been "invisible" provides a new range of conspicuity options as well as new anatomic detail that has previously been submerged in low tissue signal. Pathologic processes that might either in-

crease or decrease the signal from short T2 components (as outlined in "MR Properties of Tissues," above) have also provided a guide for the use of UTE sequences. Applications in which conventional imaging has been relatively unrewarding but in which magnetization transfer, MR spectroscopy, or other imaging techniques have shown abnormalities have been another focus of attention.

The proton signal from cortical bone probably comes mainly from the organic matrix (principally collagen), bound water, and some free water. It may provide different information than conventional radiologic methods, which mainly reflect the calcium content of the mineral component. Serial scanning shows enhancement in normal cortical bone. After intravenous gadodiamide, there was a 23% increase in signal with a peak at about 10 minutes in the study illustrated (Fig. 13).

The periosteum is well seen in many areas (Fig. 14) although there are other causes of high signal adjacent to cortical bone, and periosteum needs to be differentiated from these. Enhancement may specifically be demonstrated in the periosteum without the confounding effect of high signal from blood by the use of subtraction (Fig. 15).

High signal was consistently seen in ligaments. Local enhancement may be seen after injury (Fig. 16).

A plot of signal intensity against TE for the normal posterior cruciate ligament (PCL) before and after contrast enhancement shows that the highest baseline signal and the largest increase in signal are seen in this short T2 tissue with the shortest TE (Fig. 17).

The red (vascular) zone of the meniscus is well seen (Fig. 18). It has not been identifiable in previous studies in cadavers or patients.[29]

Regions of abnormality may be identified because they show less enhancement than that seen in normal tissue (Fig. 19). This has not previously been possible in tissues in which normal enhancement could not be visualized.

The liver shows an increased signal on difference images in hemochromatosis (Fig. 20). In cirrhosis, there is a tendency toward an increase in T2*. The fibrosis present in this condition may be associated with inflammatory change and a long T2* rather than the short T2* seen in chronic "dry" fibrosis. There may also be a loss of endoplasmic reticulum and tightly bound water reducing the concentration of short T2 components.

Tendons and muscle insertions are highlighted in the pelvis (Fig. 21). The signal may be from fibrocartilage enthases.[30]

Short T2* components can be seen in the normal white matter of the brain (Fig. 22). Applications in the brain have included conditions in which the signal from short T2* components is increased such as angiomas, malignant melanomas, calcification, and chronic gliosis as well as those in which it is

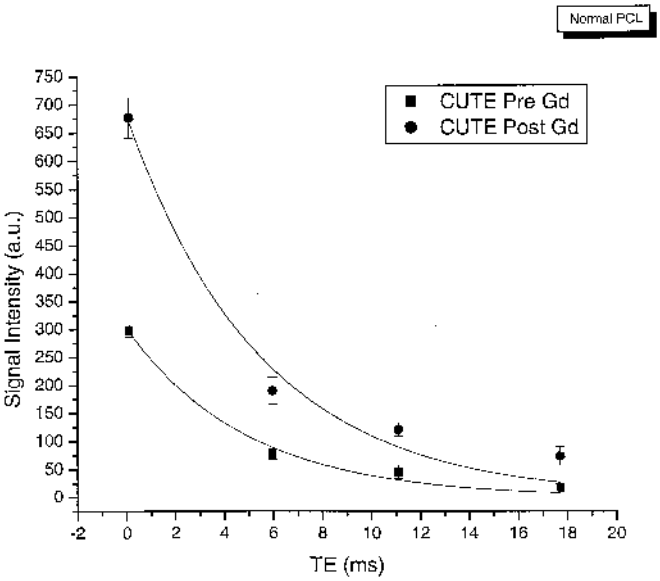

FIGURE 17. Plot of signal intensity against TE for a CUTE sequence and subsequent echoes (TR/TE = 500/0.08, 5.95, 11.08, and 17.70 milliseconds) for a normal PCL before and after contrast enhancement. The PCL shows the highest preenhancement signal and the greatest increase in signal with the shortest TE (0.08 milliseconds).

decreased such as multiple sclerosis, many tumors, and vasogenic edema. Meningeal thickening is shown in Fig. 23.

Cardiac imaging has been performed with adequate signal-to-noise ratio, and scar tissue with a short T2* has been identified as a high-signal region on difference images.

Imaging of the spine shows increased signal from ligaments and scar tissue and may show enhancement of abnormal interspinous ligaments (Fig. 24). Thalassemia is of interest as a condition in which there is premature intervertebral disc degeneration in the lower thoracic and upper lumbar spine. High-intensity bands can be seen parallel to the end plates with FLUTE sequences. These may be due to iron deposition shortening the T1 and T2 of the disc (Fig. 25).

FUTURE DEVELOPMENTS

Many further developments are possible. The process of optimization of TR, flip angle, and data sampling for different tissue T1s and T2s has only just begun. The same applies to the different long T2 signal reduction techniques. In general, fast low flip angle techniques are likely to form the basic pattern for UTE imaging. The T1s of short T2 components are generally short, which assists with fast sequences. The technique is also well suited to low flip angles to keep rf pulse durations short.

No specific developments have yet been performed on the hardware side to optimize B_1 power and to reduce rf switching times that are inadequate for some coils (at TE of 0.08 milliseconds). However, there are options already avail-

FIGURE 18. Normal knee meniscus. Sagittal d FUTE (TR/TE = 0.08 minus 17.70 milliseconds) images (A) before and (B) after enhancement. The red (vascular) zone of the meniscus is enhanced in (B) (arrows).

able for use of increased B_1 power and gradient strength with smaller dedicated transmit-receive coils and gradient sets for imaging of the brain, knee, and other parts of the body. These should allow shorter rf pulses and faster ramping to higher gradient strengths. For MR system hardware as a whole, targets for machine development of a TE of 20 microseconds, peak B_1 field of 30 μT, gradient slew rate of 200 T/m, and gradient strength of 50 T/m appear feasible.

Three-dimensional acquisitions[9] are likely to be of value in improving signal-to-noise ratio and imaging complex structures such as articular cartilage and joints with thinner slices to minimize partial volume effects. Reversed radial sampling should improve the signal-to-noise ratio for later echoes. Gradient moment nulling is likely to be of value in reducing motion artifact from later echoes.

Spiral acquisitions also proceed from the center of k-space and may provide more efficient coverage of k-space than radial sampling, although they take longer and this may lead to greater T2 decay during data collection.

There may also be sequences in which the first echo is of the UTE type, but later echoes use a conventional readout so that the sequence as a whole generates both types of image in a single acquisition. The combination of UTE gradient echoes and spin echoes for the later echoes would also remove some of the susceptibility artifacts that may be present with subtraction from the later gradient echoes. The radial approach is also compatible with partially parallel imaging techniques[31] given adequate signal-to-noise ratio. This could allow faster imaging.

An interesting feature of UTE sequences is that the center of k-space is oversampled so that the signal-to-noise ratio of low-frequency components is higher than that of high-frequency components. This may result in useful tissue contrast in particular clinical situations.

By combining UTE and magnetization transfer imaging, it may be possible to observe magnetization transfer (MT) effects due to extremely short T2 species (eg, 10 microseconds) through their effects on short, but detectable T2 species. Imaging of T1 in the rotating frame involves the use of rf pulses for times of the duration of T2 followed by conventional data collection. This may be achievable for short T2 species using UTE sequences without exceeding rf power limitations (at

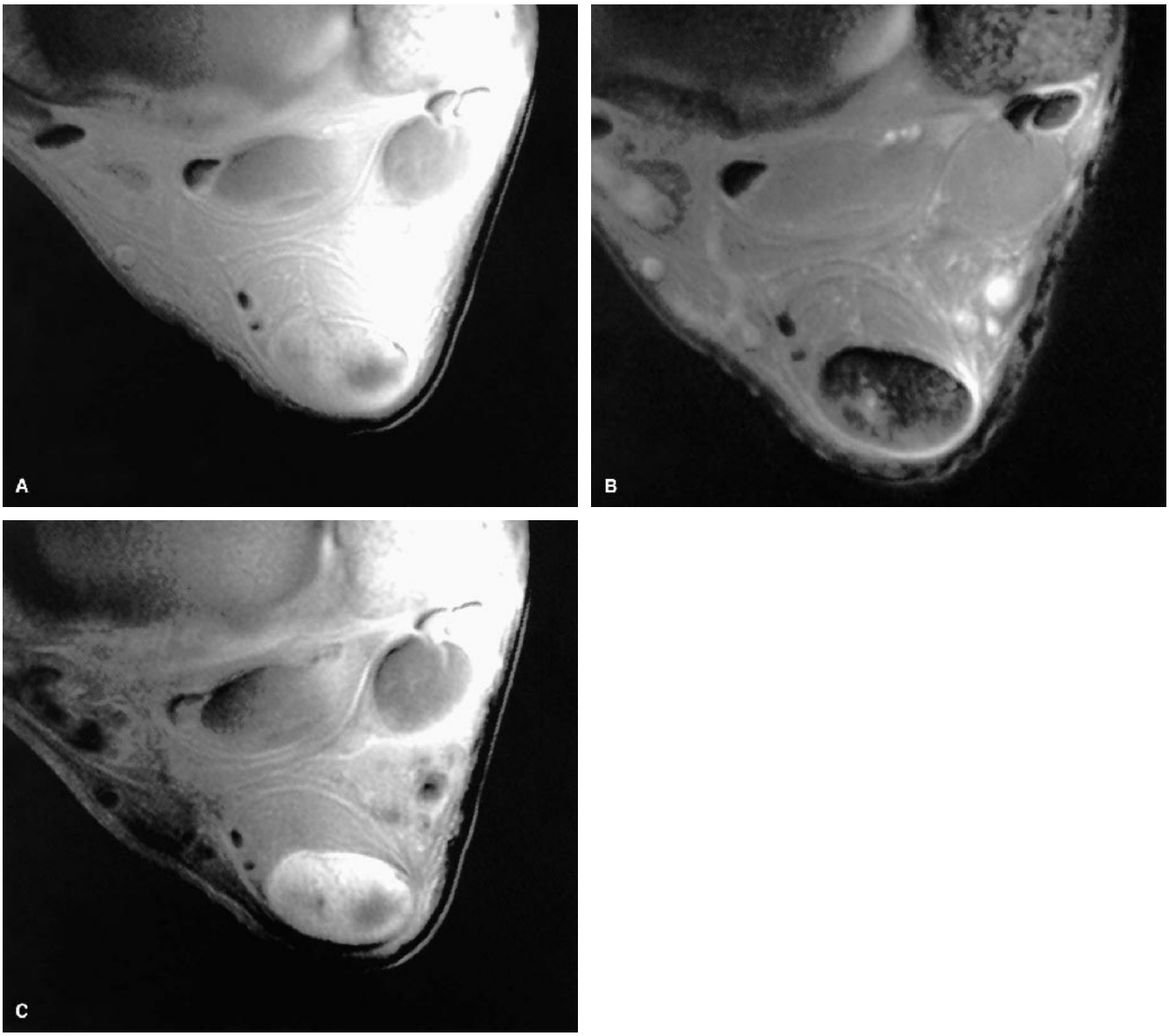

FIGURE 19. Transverse CUTE (TR/TE = 500/0.08 milliseconds) images of the Achilles' tendon after (A) contrast enhancement, (B) second echo (TR/TE = 500/5.95), and (C) d CUTE images formed from (A) minus (B). The tendon shows two low-signal areas in (A) and (C). The smaller one has an increased T2 on (B), but the other does not. The larger area has enhanced less than the surrounding normal tendon.

least at low B_o fields) and may be relevant for the study of the relaxation properties of large molecules with short T2s.

Most of this paper has been concerned with imaging of tissues, but UTE sequences are also useful for imaging of blood flow because short TEs decrease dephasing effects due to flow and can help preserve signal during turbulence.[18]

Both phosphorus and sodium have tissue components with short T2s. These nuclei are present in lower concentration than protons, but there are advantages to imaging them with UTE sequences. Radial acquisitions have been used to reduce the TE for sodium imaging to 0.3 to 0.4 milliseconds.[32,33] We have imaged sodium in tendons, ligaments, and intervertebral discs using a TE of 0.07 milliseconds and have also imaged phosphorus in cortical (Fig. 26) and trabecular bone.[34] The phosphorus in bone is in crystalline calcium phosphate and calcium hydroxy-appatite and has a T1 of 10 seconds and T2 of 0.17 milliseconds at 1.5 T. UTE chemical shift imaging (CSI) imaging has also been implemented for sodium and phosphorus studies of the heart. Hyperpolarized noble gas im-

FIGURE 20. Hemochromatosis of the liver: d FUTE image (TR/TE = 500/0.08 minus 17.70 milliseconds). The liver has a high signal intensity.

aging may also benefit from UTE studies because of the limited time for diffusion after excitation.

LIMITATIONS

Limitation can be grouped under machine, tissue, and safety headings. Machine limitations have already been alluded to. There are limits to B_1 power, gradient slew rate, and gradient strength as well as switching time. Rf power deposition increases as the reciprocal of pulse duration with a constant flip angle, which is a particular problem when short rf pulses are required. The truncated nature of the rf excitation means that the slice profile is less sharply defined than with conventional long sinc pulses. The 2 stages required for slice selection may mean that this is less robust than with conventional techniques.

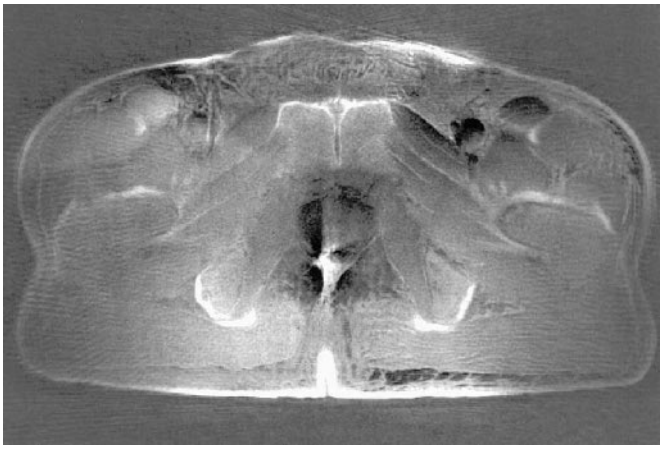

FIGURE 21. Normal pelvis: d FUTE image (TR/TR = 500/0.08 minus 5.95 milliseconds). Insertions of the rectus abdominus and the hamstring tendons have a high signal.

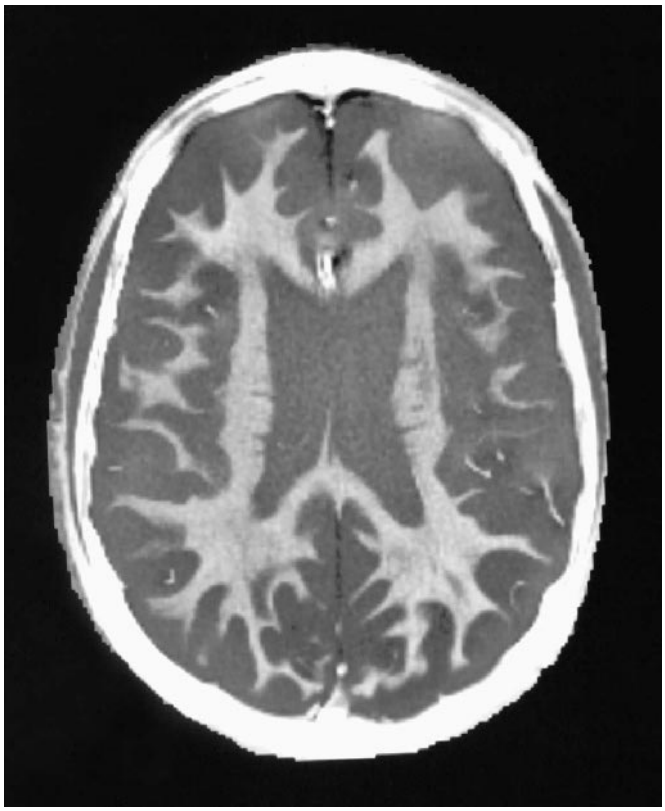

FIGURE 22. Normal brain: dl STUTE image (TR/TE/TI = 2500/0.08 minus 5.95/360 milliseconds). The long T2 components in white matter have been nulled leaving the short T2 components (mean T2 about 0.6 milliseconds) as high-signal areas.

UTE sequences also suffer from the disadvantage of requiring 2 TR periods per line of k-space (instead of 1 with conventional sequences) thus making them slower. Even then, only a single radius of k-space is mapped (as opposed to a diameter) which also increases the time required for complete mapping of k-space by a factor of 2. Radial mapping is also less effective than rectilinear mapping in terms of the density of k-space covered by a factor of $\pi/2$. Thus, for equivalent mapping of k-space, UTE imaging takes about 6 times as long as rectilinear mapping.

Fat and long T2 reduction techniques also have disadvantages (see "Image Interpretation," above).

There are also constraints due to tissue properties. Short T2 components are only present in low concentration in many tissues. Furthermore, by virtue of having a short T2, the process of useful data acquisition is limited in time. For example,

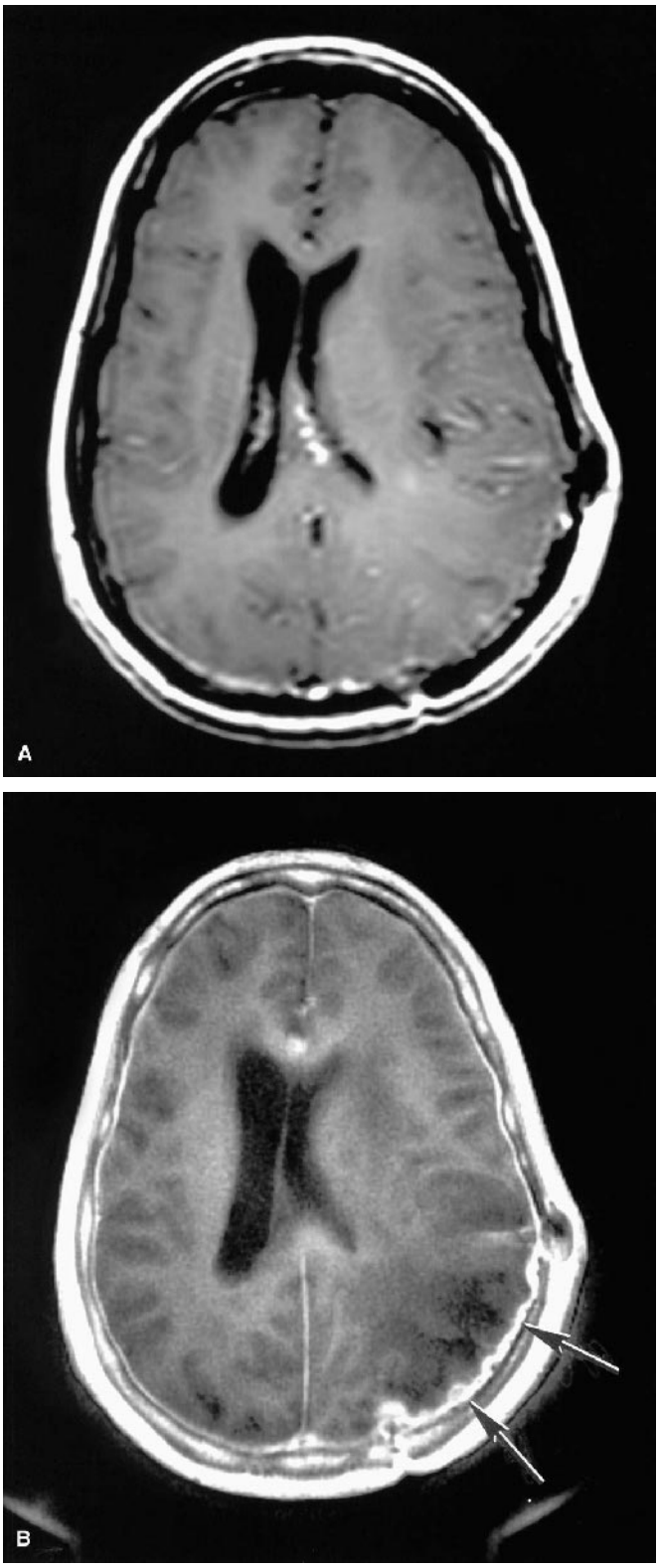

FIGURE 23. Meningeal thickening: Conventional (A) 2DFT T1-weighted (TR/TE = 500/8 milliseconds) and (B) d CUTE (TR/TE = 500/0.08 minus 5.95 milliseconds) images. Normal meninges are well seen in (B). There is thickening at the site of a previous craniotomy (arrows).

FIGURE 24. Degenerative disease of the spine. Sagittal contrast-enhanced FUTE (TR/TE = 500/0.08 milliseconds) image. Enhancement is seen in discs and scar tissue as well as the interspinous ligaments (arrows).

to image a tissue component with an extremely short T2 (eg, 10 microseconds), a data acquisition of say 10–20 points at 1-microsecond sampling intervals might be used. This could only result in a poorly resolved blur that would probably not be of diagnostic value. Biological safety concerns are related to excessive B_1 power deposition and high gradient slew rates.

Overall, these constraints tend to be manifest in clinical terms as limitations to the signal-to-noise and contrast-to-noise ratios achievable in a given time, as for example in detecting a reduction in short T2 components in a tissue in which these components are in a minority using a long T2 reduction technique.

Short TE conventional spin echo pulse sequences provide a potential method of imaging short T2 components while

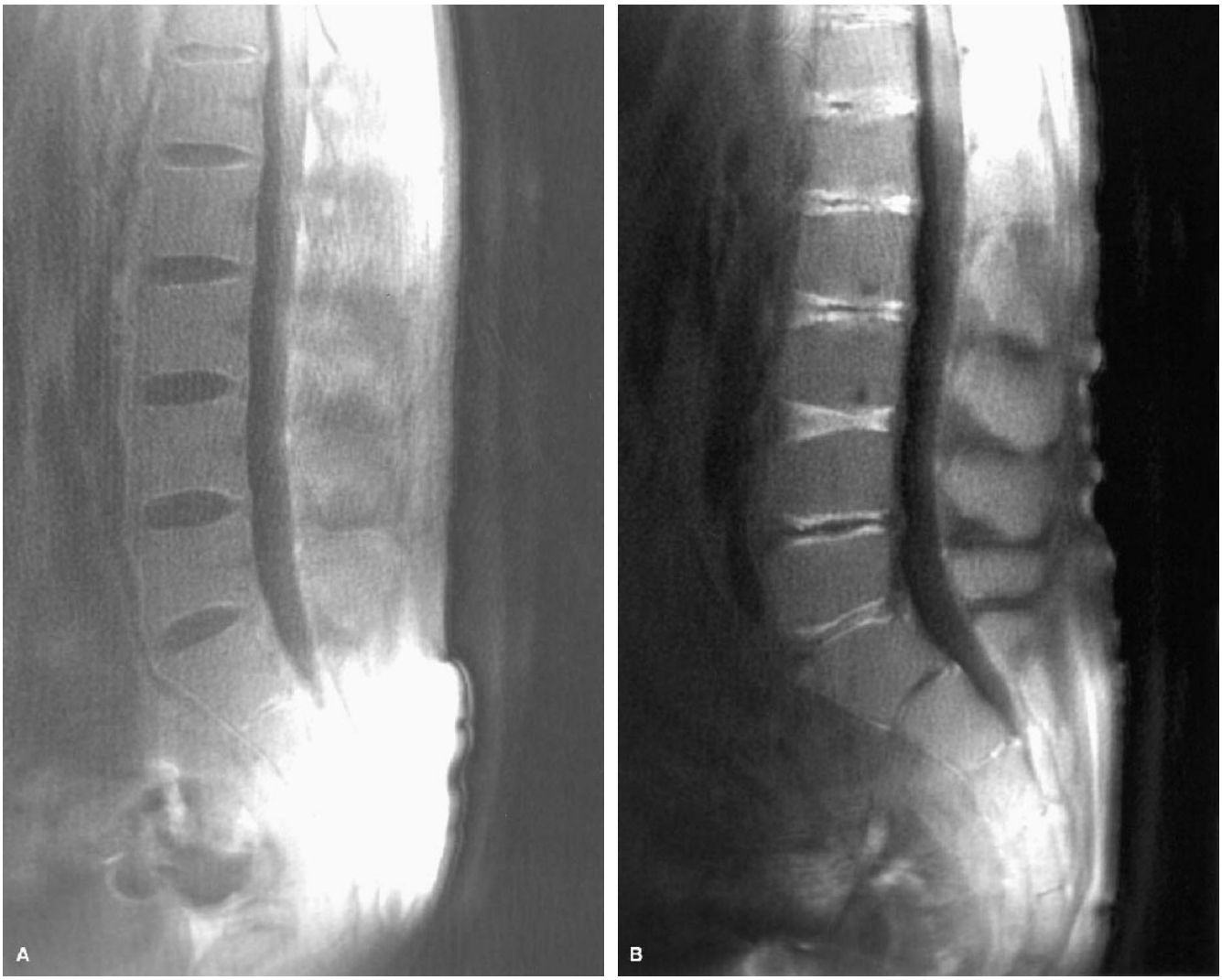

FIGURE 25. (A) Sagittal normal spine image with a FLUTE sequence (TR/TE = 500/0.08 milliseconds) and (B) patient with thalassemia imaged with the same sequence. Obvious high-signal bands are seen parallel to the end plates within the discs on (b).

minimizing susceptibility effects; however, there are limits on how far TE can be reduced. The inversion pulse needs to be short (for imaging of short T2 components) and time is required for crusher gradients on either side of it. The shortest available TE in our hands (even with a non-slice-selected inversion pulse) has been 1.3 milliseconds, which is over 15 times longer than the TEs available with UTE sequences.

CONCLUSION

UTE pulse sequences provide a new approach to imaging a group of tissues and tissue components that have previously received little attention in terms of technique development. These sequences detect short T2 components and are genuinely complimentary to conventional sequences such as fast spin echo imaging, echo planar imaging (EPI), and diffusion-weighted imaging which detect long T2 components. They also detect short T2 components that cannot be detected with conventional T1-weighted sequences.

Unlike MR as a whole, which largely proceeded from brain imaging (exploiting its long T2) to the rest of the body, clinical UTE imaging is likely to proceed initially with tissues with short T2s in the musculoskeletal system and later to more demanding applications in other systems of the body where short T2 components are in lower concentration and patient motion may be a significant constraint.

Already tendons, ligaments, menisci, cortical bone, discs, brain, and liver have been imaged in novel and interesting ways with and without contrast enhancement, but as with other developments in clinical MR, UTE sequences will re-

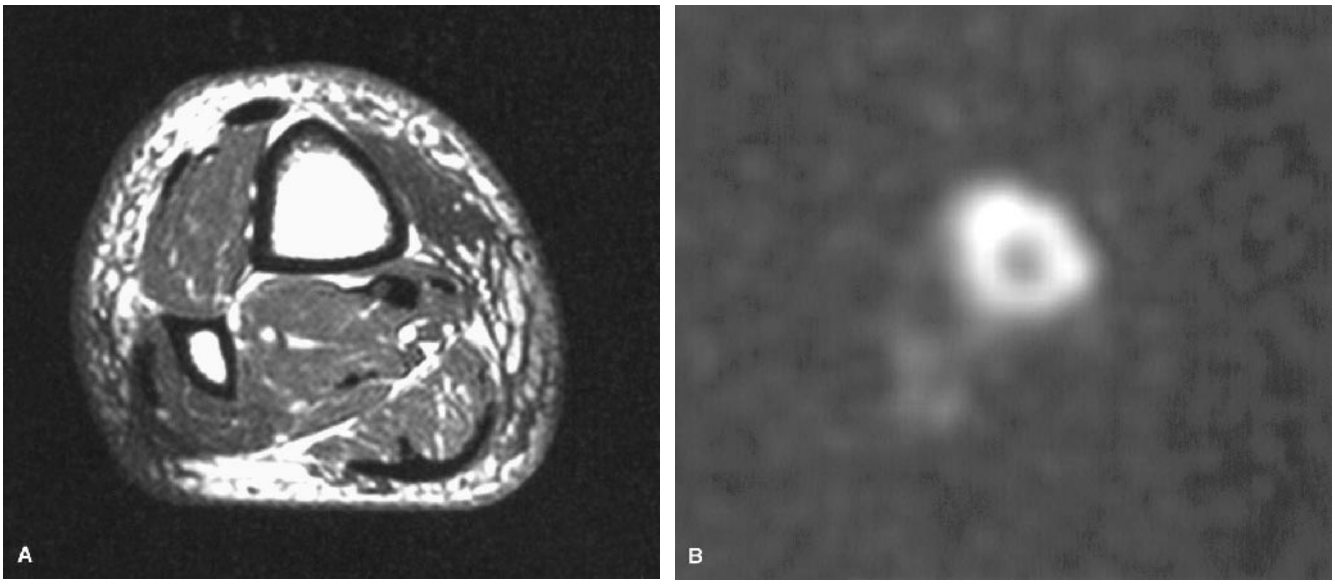

FIGURE 26. Transverse CUTE (TR/TE = 100/0.07 milliseconds) proton image of (A) the lower leg and (B) matching phosphorus image (TR/TE = 300/0.07 milliseconds) of the same region. Phosphorus signal is seen in the cortex of the tibia in (B).

quire careful evaluation and detailed comparison with other techniques to establish their clinical role.

REFERENCES

1. Smith FW. In: Witcofski RL, Karstaedt N, Partain CL, eds. *NMR Imaging*. Winston Salem, NC: Bowman Gray School of Medicine; 1982:125–132.
2. Edelstein WA, Bottomley PA, Hart HR, et al. In: Witcofski RL, Karstaedt N, Partain CL, eds. *NMR Imaging*. Winston Salem, NC: Bowman Gray School of Medicine; 1982:139–146.
3. Henkelman RM, Stanisz GJ, Graham GJ. Magnetization transfer in MRI: a review. *NMR Biomed*. 2001;14:57–64.
4. Bergin CJ, Pauly JM, Macovski A. Lung parenchyma: projection reconstruction MR imaging. *Radiology*. 1991;179:771–781.
5. Bergin CJ, Noll DC, Pauly JM, et al. MR imaging of lung parenchyma: a solution to susceptibility. *Radiology*. 1992;183:673–676.
6. Gold G, Pauly J, Moretto J, et al. Characterization of artherosclerotic plaque at 1.5T. *J Magn Reson Imaging*. 1993;3:399–407.
7. Gold GE, Pauly JM, Macovski A, et al. MR spectroscopic imaging of collagen: tendons and knee menisci. *Magn Reson Med*. 1995;34: 647–654.
8. Brossmann J, Frank LR, Pauly JM, et al. Short echo time projection reconstruction MR imaging of cartilage with histopathologic correlation: comparison with fat-suppressed spoiled GRASS and magnetization transfer contrast MR imaging. *Radiology*. 1997;203:501–507.
9. Schmidt MA, Yang GZ, Gatehouse PD, et al. FID-based lung MRI at 0.5T: theoretical considerations and practical implications. *Magn Reson Med*. 1998;39:666–672.
10. Gold GE, Thedens DR, Pauly JM, et al. MR imaging of the articular cartilage of the knee: new methods using ultrashort TE's. AJR *Am J Roentgenol*. 1998;170:1223–1226.
11. Frank LR, Wong EC, Buxton RB, et al. Mapping the physiological parameters of articular cartilage with magnetic resonance imaging. *Top Magn Reson Imaging*. 1999;10:153–179.
12. Gold GE, Wren TAL, Nayak KS. In vivo short echo time imaging of Achilles Tendon. *Proc Int Soc of Magn Reson Med*. 2001:244.
13. Nayak KS, Pauly JM, Gold GE, et al. Imaging ultrashort T_2 species in the brain. *Proc Int Soc Magn Reson Med*. 2000:509.
14. Gold GE, Pauly JM, Leung AN, et al. Short echo time MR spectroscopic imaging of the lung parenchyma. *J Magn Reson Imaging*. 2002;15:679–684.
15. Gatehouse PD, Bydder GM. Magnetic resonance imaging of short T_2 components in tissues. *Clin Radiol*. 2003;58:1–19.
16. Lu A, Grist TG, Black WF. Improved spectral selectivity and reduced susceptibility in true-FISP using a near zero TE undersampled 3D PR sequence. *Proc Int Soc Magn Reson Med*. 2002:470.
17. Reichert IHL, Gatehouse PD, Firmin DN, et al. Proton imaging of periosteum and cortical bone with ultrashort TE pulse sequences. *Proc Int Soc Magn Reson Med*. 2003:451.
18. Neilson HT, Gold GE, Olcott EW, et al. Ultrashort echo time 2D time of flight MR angiography using a half-pulse excitation. *Magn Reson Med*. 1999;41:591–599.
19. Gatehouse PD, Thomas RW, Karadaglis D, et al. Imaging of the knee with ultrashort TE (UTE) pulse sequences. *Proc Int Soc Magn Reson Med*. 2003:111.
20. Chappell KE, Gatehouse PD, Williams AD, et al. Clinical imaging of the liver with ultrashort TE pulse sequences. *Proc Int Soc Magn Reson Med*. 2003:1418.
21. Gatehouse PD, Waldman A, Van Dellen JR, et al. Clinical imaging of the brain with ultrashort TE (UTE) pulse sequences. *Proc Int Soc Magn Reson Med*. 2003:2268.
22. Pauly J, Conolly S, Macovski A. Suppression of long T_2 components for short T_2 imaging. *J Magn Reson Imaging*. 1992;2:145.
23. Harrison R, Bronskill MJ, Henkelman RM. Magnetization transfer and T_2 relaxation components in tissue. *Magn Reson Med*. 1995;33:490–496.
24. Fenrich FR, Beaulieu C, Allen PS. Relaxation times and microstructures. *NMR Biomed*. 2001;14:133–139.
25. Hayes CW, Parellada JA. The magic angle effect in musculoskeletal MR imaging. *Top Magn Reson Imaging*. 1996;8:51–56.
26. Henkelman RM, Stanisz GJ, Kim JK, et al. Anisotropy of NMR properties of tissue. *Magn Reson Med*. 1994;32:592–602.
27. Oatridge A, Herlihy AH, Thomas RW, et al. Magnetic resonance: magic angle imaging of the Achilles tendon. *Lancet*. 2001;358:1610–1611.
28. Oatridge A, Herlihy A, Thomas RW, et al. Magic angle imaging of the Achilles tendon in patients with chronic tendonopathy. *Clin Radiol*. 2003; 58:384–388.
29. Hauger O, Frank LR, Boutin RD, et al. Characterization of the "red zone"

on knee meniscus: MR imaging and histologic correlation. *Radiology*. 2000;217:193–200.
30. Benjamin M, Ralphs JR. Fibrocartilage in tendons and ligaments—an adaptation to compressive load. *J Anat*. 1998;193:481–494.
31. Pruessmann KP, Weiger M, Bornert P, et al. Advances in sensitivity encoding with arbitrary k-space trajectories. *Magn Reson Med*. 2001;46: 638–651.
32. Ouwerkerk R, Bleich KB, Gitten JS, et al. Tissue sodium concentration in human brain tumors as measured with ^{23}Na MR imaging. *Radiology*. 2003;227:529–537.
33. Thulborn KR, David D, Adams H, et al. Quantitative tissue sodium concentration mapping of the growth of focal cerebral tumors with sodium magnetic resonance imaging. *Magn Reson Med*. 1999;41:351–359.
34. Robson MD, Gatehouse PD, He T, et al. Human in vivo imaging of phosphorus in cortical bone using ultrashort TE pulse sequences. *Proc Int Soc Magn Reson Med*. 2003:791.